

Low Metallicity ISM: excess submillimetre emission and CO-free H₂ gas

Suzanne C. Madden¹, Aurélie Rémy¹, Frédéric Galliano¹, Maud Galametz², George Bendo³, Diane Cormier¹, Vianney Lebouteiller¹, Sacha Hony¹ and the *Herschel* SAG 2 consortium

¹CEA Saclay, DSM, AIM, Service d'Astrophysique, Gif-sur-Yvette 91911, France

²Institute of Astronomy, University of Cambridge, Madingley Rd., Cambridge, UK

³Alma Regional Center, University of Manchester, Oxford Rd., Manchester, UK

email: suzanne.madden@cea.fr

Abstract. The low metallicity interstellar medium of dwarf galaxies gives a different picture in the far infrared(FIR)/submillimetre(submm)wavelengths than the more metal-rich galaxies. Excess emission is often found in the submm beginning at or beyond 500 μm . Even without taking this excess emission into account as a possible dust component, higher dust-to-gas mass ratios (DGR) are often observed compared to that expected from their metallicity for moderately metal-poor galaxies. The Spectral Energy Distributions (SEDs) of the lowest metallicity galaxies, however, give very low dust masses and excessively low values of DGR, inconsistent with the amount of metals expected to be captured into dust if we presume the usual linear relationship holding for all metallicities, including the more metal-rich galaxies. This transition seems to appear near metallicities of $12 + \log(\text{O}/\text{H}) \approx 8.0 - 8.2$. These results rely on accurately quantifying the total molecular gas reservoir, which is uncertain in low metallicity galaxies due to the difficulty in detecting CO(1-0) emission. Dwarf galaxies show an exceptionally high [CII] 158 μm /CO (1-0) ratio which may be indicative of a significant reservoir of 'CO-free' molecular gas residing in the photodissociated envelope, and not traced by the small CO cores.

Keywords. galaxies: dwarf, galaxies: ISM, ISM: molecules

1. Introduction

Understanding how galaxies evolve requires fundamental comprehension of the process of star formation and the subsequent effects on the interstellar medium (ISM) under conditions in the early universe - an epoch when the ISM had not yet endured many cycles of chemical enrichment. We can attempt to extrapolate to such conditions, by studying the interplay between star formation and dust and gas in low metallicity dwarf galaxies, of which our local universe hosts a veritable zoo.

The first systematic study of dust in dwarf galaxies observed with wavelengths as long as 100 μm with *IRAS*, showed lower infrared luminosity (L_{IR}) compared to H α than spirals. $L_{12\mu\text{m}}/L_{25\mu\text{m}}$ values were lower than spirals, while the higher $L_{60\mu\text{m}}/L_{100\mu\text{m}}$ highlighted the presence of warmer dust and enhancement of very small grains (e.g. Hunter *et al.* 1989; Melisse & Israel 1994). The *ISO* and *Spitzer* missions opened up the window onto MIR spectroscopy, demonstrating the dearth of PAHs in dwarf galaxies, a consequence of the prevailing hard radiation field, shocks or delayed injection by AGB stars (e.g. Madden *et al.* 2006; Wu *et al.* 2006; O'Halloran *et al.* 2008; Galliano *et al.* 2008) as well as cooler dust revealed by longer wavelengths, extending to 160 μm (e.g. Popescu *et al.* 2002). SCUBA/JCMT and Laboca/APEX observations exposed excess emission in dwarf galaxies at 850/870 μm which, if interpreted as cold dust, could comprise a large

amount of dust in low metallicity galaxies compared to their measured gas reservoirs and their low metallicities (e.g. Galliano *et al.* 2003; Galliano *et al.* 2005; Zhu *et al.* 2009; Galametz *et al.* 2011). One constraint on the dust mass should be the measured dust-to-gas mass ratio (DGR), as this parameter should be effected by chemical evolution. Atomic gas is often widespread in dwarf galaxies, in contrast to molecular gas, if the CO(1-0) is a reliable tracer of the molecular reservoir in these galaxies. On the other hand, the $158\ \mu\text{m}$ [CII], often assumed to arise from the photodissociation regions (PDRs) around molecular clouds, is excessively bright in dwarf galaxies compared to the CO, in contrast to more metal-rich galaxies (Poglitsch *et al.* 1995; Israel *et al.* 1996; Madden *et al.* 1997; Madden 2000). What is this telling us about the total molecular gas reservoir, the galaxy morphology and the distribution of the various gas phases in dwarf galaxies?

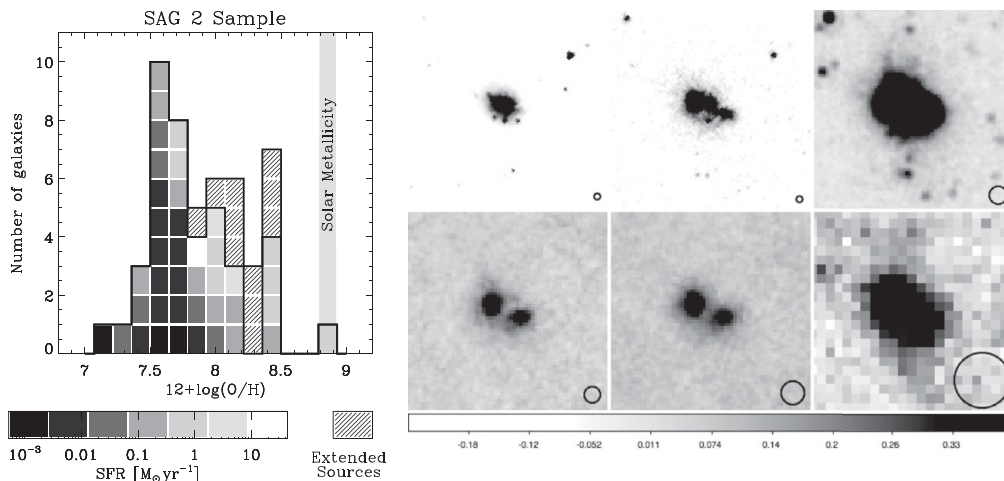


Figure 1. (left) Metallicity and star formation properties of the Herschel Dwarf Galaxy Survey. (right) *Spitzer* and *Herschel* images of the dwarf galaxy, NGC 1705. Images from left to right and top to bottom are: $3.6\ \mu\text{m}$ *Spitzer*/IRAC, $8\ \mu\text{m}$ *Spitzer*/IRAC, $24\ \mu\text{m}$ *Spitzer*/MIPS, $70\ \mu\text{m}$ *Herschel*/PACS, $100\ \mu\text{m}$ *Herschel*/PACS, $250\ \mu\text{m}$ *Herschel*/SPIRE. Image sizes are $130'' \times 130''$ and beam sizes are indicated in lower right corner of images.

Herschel has opened up the submm wavelength window beyond $160\ \mu\text{m}$, with observations covering the 50 to $500\ \mu\text{m}$ window. The Dwarf Galaxy Survey (DGS) is a *Herschel* key program targeting 48 local universe dwarf galaxies with a wide range of star formation properties and metallicity values, as low as $1/50\ Z_{\odot}$ (Fig. 1) and as nearby as the Magellanic Clouds to study the multiphase components of the stars, gas and dust under low metallicity environments.

2. SED models of dwarf galaxies

PACS observations cover 3 photometric bands: 70 , 100 and $160\ \mu\text{m}$ (FWHM $\sim 10''$; Poglitsch *et al.* 2010) while SPIRE observes at 250 , 350 and $500\ \mu\text{m}$ (FMHM= $18''$ to $38''$; Griffin *et al.* 2010). Comparison of the *Spitzer* $24\ \mu\text{m}$ images (Bendo *et al.* 2012) with the PACS $70\ \mu\text{m}$ and SPIRE $250\ \mu\text{m}$ (Fig. 1) highlights the extent of the cooler dust traced by the $250\ \mu\text{m}$ emission in contrast to the warmer dust emitting at $24\ \mu\text{m}$, favoring the more compact HII regions. Coverage at *Spitzer* and *Herschel* wavelengths provides well-sampled SEDs for wide-ranging studies of the dust properties in dwarf galaxies.

Metallicity and β and T effects. The FIR-submm behavior of the DGS sample is investigated via *Spitzer* and *Herschel* colour-colour diagrams, to obtain an overview of the

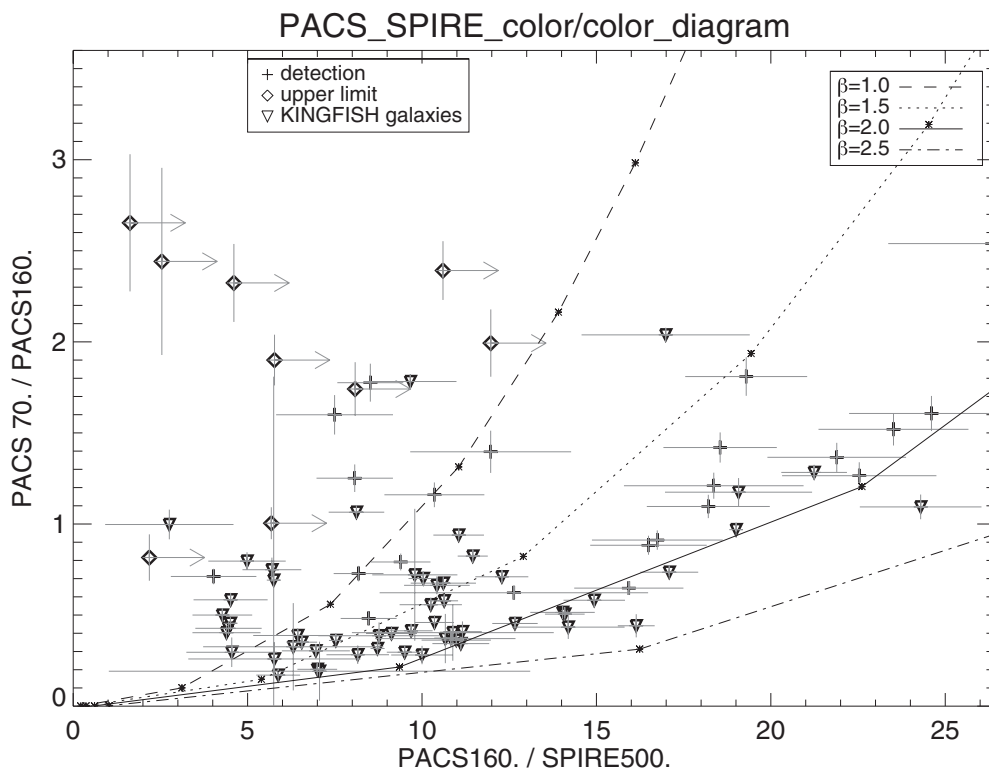


Figure 2. Herschel colour-colour diagram of DGS galaxies detected in at least all PACS bands: PACS70/160 and PACS160/SPIRE500. For comparison, KINGFISH galaxies (Dale *et al.* 2012) are also shown (downward triangles). Modeled modified black body fits with $\beta = 1.0, 1.5, 2.0, 2.5$ are shown in curves, with temperature values noted as dots on the curves, increasing from 10 K in steps of 10 K, starting from the lower left of the curves to the upper right.

total sample (Rémy *et al.* in preparation; also this volume). Fig. 2 shows the effect of varying emissivity indices (β) and average dust temperatures (T) presuming a single modified black-body to explain the FIR-submm emission. For comparison the KINGFISH galaxies (Dale *et al.* 2012) are also included. The effect of the overall higher metallicity clusters the bulk of the KINGFISH sample between $\beta = 1.5$ and 2.0. The most active dwarf galaxies, particularly the blue compact dwarfs, peak at wavelengths less than $70 \mu\text{m}$ and some between 35 and $60 \mu\text{m}$, much shorter wavelengths compared to the more metal-rich starburst galaxies. The difference in the shape of the SEDs of dwarf galaxies can be noted via the *Herschel* colour-colour diagram: as a consequence of their overall hotter dust peaking at MIR wavelengths (higher PACS70/PACS160 values for the lower metallicity bins), their Rayleigh-Jeans slope drops off at FIR and submm wavelengths. Consequently, these galaxies are often not detected at all SPIRE wavelengths for the lowest metallicity galaxies, particularly at $500 \mu\text{m}$. A prominent example of this effect is illustrated in one of the lowest metallicity galaxies of our sample, SBS0335-052E ($12+\log(\text{O}/\text{H}) = 7.29$; Fig. 3). The integrated SED shows the flatter MIR-FIR emission peaking between 20 and $30 \mu\text{m}$ (Houck *et al.* 2004; Galliano *et al.* 2008; Sauvage *et al.* in preparation). The very dense super star clusters dominate the warm overall dust emission, with the observed SED leaving little evidence for cold submm-emitting dust.

For those dwarf galaxies detected at both PACS and SPIRE wavelengths, modified black-body fits (omitting $70 \mu\text{m}$ in the fits) give a wide range of β and T solutions with

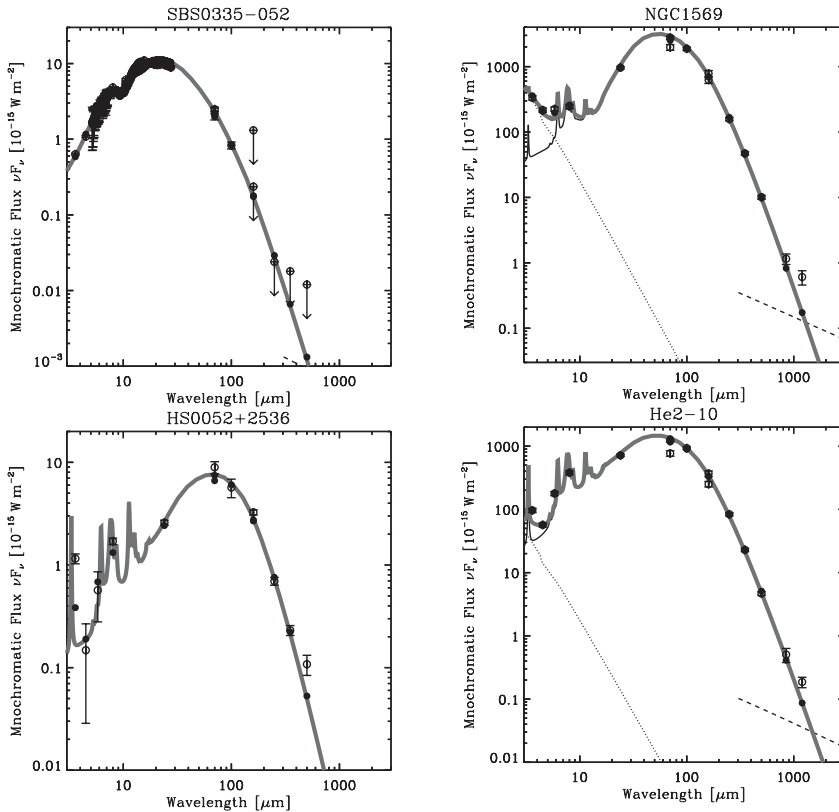


Figure 3. SEDs of dwarf galaxies. SBS0335-052 has on average very hot dust, with the SED peaking between 20 and 30 μm (Galliano *et al.* 2008; Sauvage *et al.* in preparation). HS0052+2536 shows a very low β in the *Herschel* colour-colour diagram (Fig. 2) and does indeed show a 500 μm excess. NGC 1569 and He2-10 both fall near $\beta \sim 2$ in the colour-colour diagram, but their full SED model unveils an excess *beyond* 500 μm . *Spitzer* and *Herschel* data are used to constrain the SED models. *Herschel* observations are used for the model constraints in the cases of data redundancy (70 and 160 μm). Stellar contribution is shown as dotted lines, the dashed lines are the free-free continuum, extrapolated from observed radio observations when available and the solid grey curve is the total modeled SED. The open squares are the observations while the black points show the predicted model fluxes, often overlapping completely with the open squares.

a mean β of 1.6 and mean T of 32 K (Fig. 4). Since the most metal-poor galaxies of the DGS sample do not have 500 μm detections, this distribution of modeled β and T is primarily representing galaxies with metallicity values greater than $12 + \log(\text{O}/\text{H}) \sim 8.0 - 8.2$. For comparison, the KINGFISH galaxies show a similar mean β but the T distributions are cooler, peaking between ~ 20 and 25 K (Dale *et al.* 2012). Galaxies requiring an exceptionally low β solution, may be indicative of the presence of a submm excess which could start to be detectable at wavelengths as low as 500 μm .

Submm excess examples. Taking into account the optical to submm and radio wavelengths, full SED models (Galliano *et al.* 2008) can help to further interpret the *Herschel* colour-colour diagrams. For example, from the *Herschel* colour-colour diagram (Fig. 2), HS0052+2536 has an exceptionally low β value ~ 1 . Inspection of the fully modeled SEDs (Fig. 3) shows that a submm excess is indeed present. About 50% of the DGS galaxies detected at 500 μm show a submm excess of $\sim 7\%$ to 100% above the SED model (R my *et al.*, in preparation). A relationship between metallicity and submm excess within the

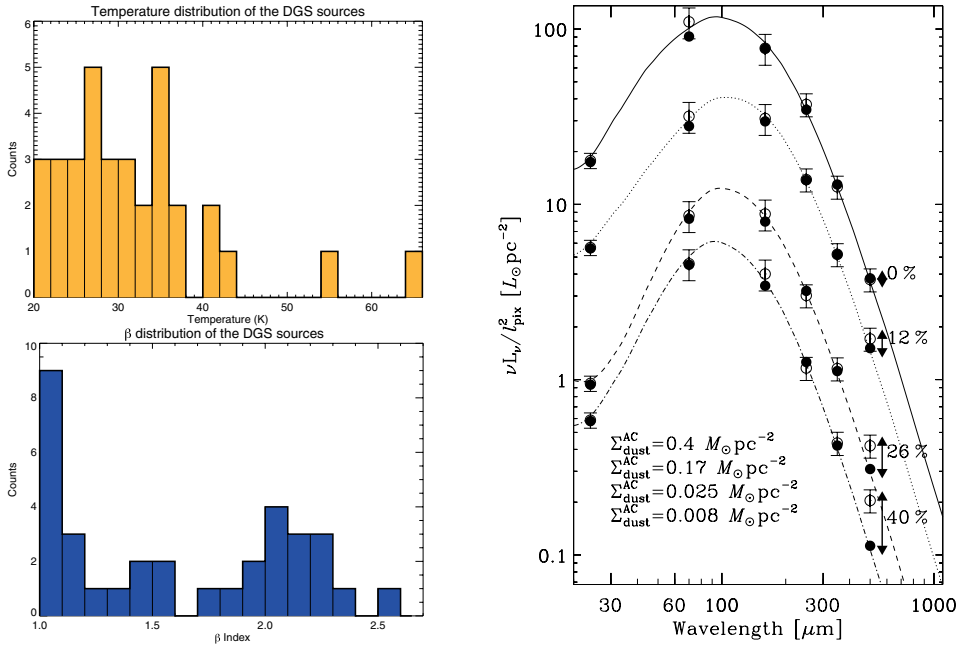


Figure 4. (left) T and β distribution of the DGS sample with 500 μm detections. (right) Selected SEDs in the LMC showing submm excess ranging up to 40% compared to that expected from the SED models (Galliano *et al.* 2011). SEDs are for a range of dust mass surface densities, ranging from the lowest to the highest values, corresponding to lower to higher profiles, respectively.

DGS sample is not yet obvious. This may be somewhat due to the requirement for 500 μm detections which often omits the lowest metallicity galaxies. While this *Herschel* colour-colour diagram highlights potential galaxies with submm excess, galaxies for which the excess begins beyond 500 μm will be missed without observations at longer wavelengths. For example, NGC 1569 and He2-10, show $\beta \sim 2$ in the *Herschel* colour-colour diagram but do indeed show a submm excess when including their ground-based 850 μm observations (Fig. 3; see also Galliano *et al.* 2003; Galliano *et al.* 2005; Galametz *et al.* 2011).

DGRs and possible origins of the submm excess. Understanding how the DGR varies as a function of metallicity is important to have an accurate picture of the gas and dust life cycle in galaxies. How are the heavy metals incorporated into dust and how do metallicity or other local or global parameters control this process? Understanding the behavior of the DGR is also important since many studies determining the dust mass in galaxies then quantify the gas reservoir in galaxies by assuming a DGR. Numerous studies have noted a proportionality of DGR with metallicity, but results can vary depending on the long wavelength data used. Engelbracht *et al.* (2008) noted a decrease in DGR from the more metal rich galaxies to the moderately metal-poor galaxies, until $12 + \log(\text{O}/\text{H}) \sim 8$, beyond which the DGR appears to be constant. Adding 850 μm observations beyond *Spitzer* wavelengths, however, can increase dust masses (Galametz *et al.* 2011). The low metallicity end of the DGR relationship has been particularly ambiguous, since dust mass estimates of dwarf galaxies are sometimes hampered by a submm excess.

For the lowest metallicity galaxies ($12 + \log(\text{O}/\text{H}) < 8.0$) where the overall SED peaks at short wavelengths and where we have mostly only upper limits in the submm, we find low upper limits to dust masses and low DGRs compared to the expected value. The upper limit dust mass from SBS0335-052, for example, is very low (Galliano *et al.*

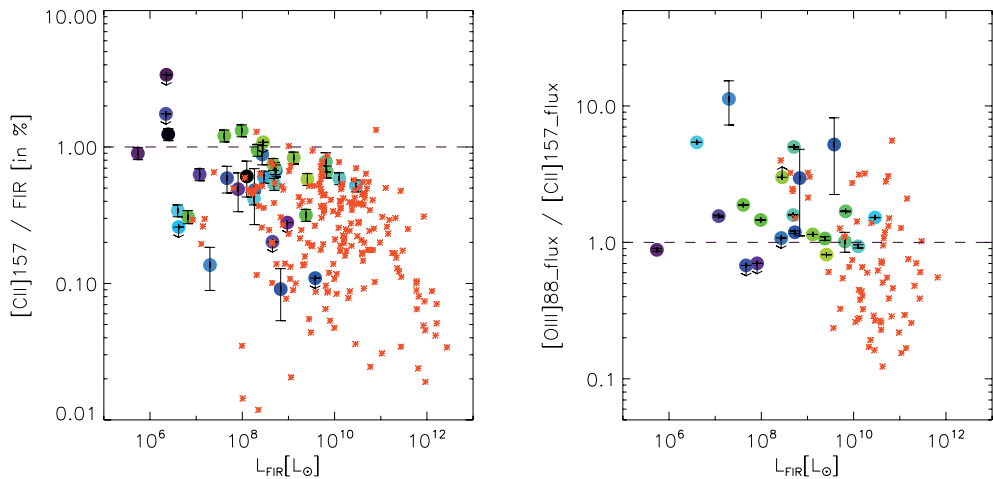


Figure 5. [CII]/FIR and [OIII]/FIR as a function of $L_{[FIR]}$ for the DGS sample (large dots) compared to that of Brauher *et al.* 2008 ISO data (small squares) - mostly metal-rich galaxies.

2008; Sauvage *et al.* in preparation) giving an unusually low total DGR, compared to that expected for its extremely low metallicity. The low DGR measured for the lowest metallicity galaxies may be telling us that perhaps metals are not necessarily incorporated into dust in the same way for the lowest metallicity galaxies as for the more metal rich galaxies. On the other hand, perhaps the total gas reservoir is underestimated.

The submm excess has been noted in dwarf galaxies for almost 10 years now - since the first SCUBA observations of dwarf galaxies at $850 \mu\text{m}$. Yet the origin remains uncertain. In the LMC, where Herschel brings 10 pc resolution at $500 \mu\text{m}$, Galliano *et al.* (2011) (see also Galliano, this volume) have highlighted locations of submm excess ranging from 15% to 40% compared to that expected from the SED models (Fig. 4). The excess seems to be anticorrelated with the dust mass surface density. Possible explanations for the submm excess include: 1) very cold dust component (e.g. Galliano *et al.* 2005; Galametz *et al.* 2011; 2) excessive free-free emission; 3) unusual dust emissivity properties (e.g. Lisensfeld *et al.* 2002; Mény *et al.* 2002; Galliano *et al.* 2011; Paradis *et al.* 2012); 4) anomalous spinning dust (e.g. Draine & Lazarian 1998; Ysard *et al.* 2010). With more sensitive submm wavelength coverage, *Herschel* is confirming the flatter submm slope in more dwarf galaxies. Problems exist with these explanations put forth for the origin of the excess. For example, invoking a very cold dust component to account for the submm excess can augment the dust mass excessively, resulting in a *very high DGR* compared to that expected for the metallicity. But, are we correctly quantifying the total molecular gas mass in low metallicity environments?

3. The molecular gas in dwarf galaxies

While CO is the widely used means to access M_{H_2} in galaxies, it is by now a well-established fact that the Galactic X factor, which converts CO to M_{H_2} , underestimates the mass of molecular gas in low metallicity galaxies. What is uncertain, however, is how to accurately correct up this factor as a function of metallicity to obtain the total gas reservoir. During the last 2 decades valiant effort has been invested in detecting and interpreting CO emission in low luminosity dwarf galaxies to quantify the molecular gas reservoir (e.g. Leroy *et al.* 2009 and references within). With the first detections of the $158 \mu\text{m}$ [CII] line in dwarf galaxies on the KAO, the surprisingly high [CII]/CO values

highlighted the fact that CO could be missing a large reservoir of molecular gas (factors of 10 to 100) due to the lower dust abundance. The consequently deeper penetration of UV photons further photodissociate CO, reducing the CO cores - hence, the dearth of detected CO. Due to the self-shielding of H₂, the larger C⁺-emitting envelope can harbor H₂ which is not accounted for via CO observations (e.g. Poglitsch *et al.* 1995; Madden *et al.* 1997; Wolfire *et al.* 2010). The observed [CII]/CO, thought to be a useful tracer of star formation in galaxies, can sometimes be a factor of a 2 to 5 (or more) times higher in dwarf galaxies than in metal-rich galaxies (e.g. Madden 2000; Stacey *et al.* 2010).

Dwarf galaxies generally emit a larger fraction of their FIR in the [CII] line, ~ 0.5 to 2 %, in contrast to the more metal-rich spirals and starbursts which usually show [CII]/FIR less than $\sim 0.5\%$ (Fig. 5). If [CII] is the dominant coolant in galaxies and the photoelectric effect is responsible for the primary heating of the ISM, then [CII]/FIR can be thought of as a proxy for the grain photoelectric heating efficiency (e.g. Rubin *et al.* 2009) – the fraction of the power being absorbed by the grains that goes into heating of the ISM. The high [CII]/FIR values observed in dwarf galaxies thus, imply high photoelectric heating efficiencies which may be attributed to properties of the low-metallicity ISM, including lower dust abundance, clumpy ISM, etc. Traversing the galaxy, UV photons suffers less attenuation in the metal-poor ISM, and as a consequence of the longer photon mean-free path, the dust on galaxy-wide scales is subject to lower UV flux, effectively decreasing the overall FIR flux and increasing the observed [CII]/FIR. The 88 μm [OIII] line is typically the brightest FIR line in dwarf galaxies - usually brighter than the [CII] line (Fig. 5), normally considered to be the brightest FIR line in galaxies. This suggests a substantial filling factor of ionised gas in dwarf galaxies and places an important constraint on quantifying the origin of the [CII] line, which also can be excited by electrons in the diffuse ionized gas, not only PDRs (Lebouteiller *et al.* 2012). The [CII] and [OIII] together are important calibrators of star formation activity and characterize the diffuse and molecular phases in galaxies. With ALMA, these lines are valuable accessible diagnostics of the ISM of high red-shift galaxies offering new insight on the evolution of the star formation and ISM throughout earlier epochs.

References

- Bendo, G., Galliano, G., & Madden, S. C. 2012, *MNRAS* submitted
 Brauher, J. R. Dale, D. A., & Helou, G. 2008, *ApJS*, 178, 280
 Dale, D. A., Aniano, G., Engelbracht, C. W., Hinz, J. L., Krause, O. *et al.* 2012, *ApJ*, 745, 95
 Draine, B. T. & Lazarian, A. 1998, *ApJ*, 508, 157
 Engelbracht, C. W., Rieke, G. H., Gordon, K. D., Smith, J.-D. T. *et al.* 2008, *ApJ*, 678, 804
 Galametz, M., Madden, S. C., Galliano, F., Hony, S., Bendo, G. J. *et al.* 2011, *A&A*, 532, 56
 Galliano, F., Madden, S. C., Jones, A., Wilson, C., *et al.* 2003, *A&A*, 407, 159
 Galliano, F., Madden, S. C., Jones, A. P., Wilson, C. D., & Bernard, J.-P. 2005, *A&A*, 434, 867
 Galliano, F., Dwek, E., & Chantal, P. 2008, *A&A*, 672, 214
 Galliano, F., Hony, S., Bernard, J.-P., Bot, C., Madden, S. C. *et al.* 2011, *A&A*, 536, 88
 Griffin, M., Abergel, A., Abreu, A., Ade, P. A. R. *et al.* 2010, *A&A*, 518, 3
 Houck, J. R., Charmandaris, V., Brandl, B. R., Weedman, D. *et al.* 2004, *ApJS*, 154, 211
 Hunter, D. A., Gallagher, J. S., III, Rice, W. L., *et al.* 1989, *A&A*, 336, 152
 Israel, F. P., Maloney, P. R., Geis, N., Herrmann, F., Madden, S. C. *et al.* 1996, *ApJ*, 465, 738
 Lebouteiller, V., Cormier, D., Madden, S. C., *et al.* 2012, *A&A*, submitted
 Leroy, A. K., Walter, F., Bigiel, F., Usero, A., Weiss, A. *et al.* 2009, *AJ*, 137, 4670
 Lisenfeld, U., Israel, F. P., Stil, J. M., & Sievers, A. 2002, *A&A*, 382, 860
 Madden, S. C., Poglitsch, A., Geis, N., Stacey, G. J., & Townes, C. H. 1997, *ApJ*, 483, 200
 Madden, S. C. 2000, *NewAR*, 44, 249

- Madden, S. C., Galliano, F., Jones, A. P., & Sauvage, M. 2006, *A&A*, 446, 877
Melisse, J. P. M. & Israel, F. P. 1994, *A&A*, 285, 51
Mény, C., Gromov, V., Boudet, N., Bernard, J.-Ph., *et al.* 2007, *A&A*, 468, 171
O'Halloran, B., Madden, S. C., & Abel, N. P. 2008, *ApJ*, 681, 1205
Paradis, D., Paladini, R., Noriega-Crespo, A., Mény, C. *et al.* 2012, *A&A*, 537, 113
Poglitsch, A., Krabbe, A., Madden, S. C., Nikola, T., Geis, N. *et al.* 1995, *ApJ*, 454, 293
Poglitsch, A., Waelkens, C., Geis, N., Feuchtgruber, H. *et al.* 2010, *A&A*, 518, 1
Popescu, C. C., Tuffs, R. J., Völk, H. J. *et al.* 2002, *ApJ*, 567, 221
Rubin, D., Hony, S., Madden, S. C., Tielens, A. G. G. M. *et al.* 2009, *A&A*, 494, 647
Stacey, G. J., Hailey-Dunsheath, S., Ferkinhoff, C., Nikola, T. *et al.* 2010, *ApJ*, 724, 957
Wolfire, M. G., Hollenbach, D., & McKee, C. F. 2010, *ApJ*, 716, 1191
Wu, Y., Charmandaris, V., Hao, L., Brandl, B. R., *et al.* 2006, *ApJ*, 639, 157
Ysard, N., Miville-Deschênes, M. A., & Verstraete, L. 2010, *A&A* 509, 1
Zhu, M., Papadopoulos, P., Xilouris, *et al.* 2009, *ApJ*, 706, 941

Discussion

CHAKRABARTI: The low β values you are finding would suggest considerable grain growth. This would happen only in regions of very high density. If you used a range of temperatures (instead of a single temperature), I suspect you would find that you could fit the SEDs with $\beta = 2$.

MADDEN: The Herschel colour-colour plots I presented with overlays based on modified Black-Body fits are only suggestive in locating the potential flatter submm slopes we are seeing in low metallicity galaxies. The actual modelled SEDs I showed incorporate the sophisticated SED models of Galliano *et al.* and do indeed solve for the wide range of dust temperatures.

GALLAGHER: Dwarfs contain cold HI clouds, e.g. the Young & Lo studies of yore as well more recent SMC studies. Do these clouds show up as [CII] sources as one might expect/hope?

MADDEN: These cold HI clouds of narrow velocity are tracing the cold Neutral medium and would be good candidates for [CII] detection. It would be a good experiment for Herschel.